Journal of the Korean Chemical Society
2006, *Vol. 50, No. 2*
Printed in the Republic of Korea

전기화학적으로 형성된 알파 상 니켈 수산화물의 층간 거리에 미치는 음이온의 영향 연구

V. Ganesh Kumar · 배상원† · 이재성† · 남경완 · 김광범*
연세대학교 금속공학과
†포항공과대학교 화학공학과
(2005. 10. 18 접수)

Contraction of Alpha-nickel Hydroxide Layers by Excess Coulombic Attraction of Anions

V. Ganesh Kumar, S. W. Bae†, J. S. Lee†, K. W. Nam, and K. B. Kim*
Department of Metallurgical Engineering, Yonsei University, Seodaemoon-gu, Seoul 120-749, Korea
†Department of Chemical Engineering, Pohang Institute of Science and Technology, Pohang, Korea
(Received October 18, 2005)

요 약. 본 연구에서는 전기화학적인 방법을 사용하여 Pt와 Ni 기판 상에 니켈 나이트레이트 용액을 사용하여 박막 형태의 알파 상 니켈 수산화물을 형성한 후 층간 존재하는 음이온의 종류와 농도에 따라 층상구조물의 층간 거리에 대해여 조사하였다. 층간 존재하는 나이트레이트 음이온과 양전하를 가진 층 사이의 정전 인력에 의하여 층간 거리(d_{003})는 층간 음이온의 농도에 역비례 하는 것으로 관찰되었으며, 특히 FT-IR 분석을 통하여 층간 거리가 감소한 경우 hydrogen-bonded OH만이 존재함을 확인하였다. GC-MS 분석 결과, 본 연구에 니켈 나이트레이트 용액을 사용하였음에도 불구하고 층간에 많은 량이 카보네이트 이온이 존재하는 것으로 조사되었다.

주제어: 전기화학적 석출, 알파 상 니켈 수산화물, 니켈 나이트레이트 용액, 층간 거리

ABSTRACT. Alpha Nickel hydroxide samples have been synthesized by electrodeposition on platinum and nickel substrates at current densities of 1, 5, 6, 7 and 10 $mAcm^{-2}$ at a controlled temperature of 30.00 °C from $Ni(NO_3)_2$ bath. Platinum substrate shows a tendency to incorporate less nitrate ions with increase in current density thus producing less hydroxy-deficient nickel hydroxide layers. On the whole the interlayer distance (d_{003}) is found to be inversely proportional to the amount of nitrate ions incorporated in-between the lattice. For the first time we have observed a decrease in lattice spacing with increase in concentration of intercalant (anions) and the reason for lattice contraction is attributed to the columbic attractive forces exerted by the oppositely charged nitrate ion and positively charged slabs. The Infrared spectra of the samples with expanded interlayers show two types of OH vibrations corresponding to hydrogen bonded and non-hydrogen bonded OH groups whereas the contracted interlayers show only hydrogen-boded OH groups. Although the faradaic efficiency is found to increase with increase in applied current there is a local minimum at 6.0 $mAcm^{-2}$ current density on both platinum and nickel substrates. In this manuscript, GC-MS data is provided which clearly demonstrates the electrodeposited nickel hydroxide sample to consist of huge amount of carbonate ions although the electrolyte solution in nickel nitrate.

Keywords: Alpha Nickel Hydroxide, Nitrate Bath, Anion-deficient Layers, Interlayer Spacing, GC-MS

INTRODUCTION

Nickel hydroxide finds application in alkaline batteries as cathode and also in electrochromic device as coloring material.[1-4] The material undergoes reversible solid-state redox process involving proton insertion/deinsertion between $Ni(OH)_2$ and NiOOH. It crystallizes in brucite structure involving layers or slabs considered as the main feature Nickel hydroxide has two important modifications namely α-nickel hydroxide and β-nickel hydroxide which are widely studied for more than five decades since they differ in structure and hence electrode properties.

In brief, b-nickel hydroxide, crystallizes in rhombohedral lattice with unit-cell lattice parameters of a =3.12 A° and c=4.605 A°. On the other hand, α-nickel hydroxide is a hydrated compound with chemical formula of $Ni(OH)_2$. 0.75 H_2O and crystallizes in similar rhombohedral lattice with unit-cell parameters of a=3.08 A° and c=23.41 A°. The a-form has large interlayer spacing of 7.60 A° arising from its d_{003} planes, whereas β-form offers layers which are just apart by 4.61 A° arising from d_{001} planes. Upon oxidation the a-nickel hydroxide converts to γ-nickel oxyhydroxide and β-nickel hydroxide to β-nickel oxyhydroxide. The theoretical specific capacity of α-γ couple is 456 $mAhg^{-1}$ as compared to 289 $mAhg^{-1}$ for β-β couple based on 1.6 and 1.0 e^-s reversibly exchanged during the redox reactions respectively.[5,6] Many research efforts are aimed at synthesizing alkali-stable α-nickel hydroxide since it undergoes easy transformation to β-form in battery electrolyte namely alkali.

There are many works concerning synthesis of stable α-nickel hydroxide phases such as aluminum-substituted α-$Ni(OH)_2$ and demonstrating their electrochemical advantage in reversible charge storage.[7,8] Stabilized α-nickel hydroxide electrodes have been fabricated by electrochemical impregnation as well and proved for its superior electrochemical behavior.[9] The electrochemical impregnation method involves cathodic polarization of the deposition-substrate in nickel nitrate bath which results in excess concentration of hydroxyl ions at the substrate surface due to nitrate-ion reduction and hence precipitation of the nickel hydroxide at local high-pH.

The electrochemical impregnation experiments could be broadly divided into two kinds (i) low current density (~1 $mAcm^{-2}$) deposition which provides beta-phase and (ii) high current density (>20 $mAcm^{-2}$) deposition which provides alpha-phases.[10] Interestingly electrochemically deposited α-nickel hydroxide differs from chemically synthesized α-nickel hydroxide with respect to general chemical composition mainly arising from the nitrate ions coming from the deposition bath. The electrodeposit consists of positively-charged hydroxy-deficient layers of nickel-hydroxide which are charge-compensated by an equal amount of nitrate-ions incorporated in between the layers.[11] Additionally water molecules are also incorporated. The general formula of these electrodeposited α-nickel hydroxides are given by $Ni(OH)_{2-x}(NO_3)_x \cdot yH_2O$ where x and y are the amount of nitrate ions and water molecules incorporated in the structure.

In this manuscript we have carried out careful synthesis of electrodeposits in the middle-range of small current densities on nickel and platinum substrates. The structural features of the samples inform the phases to be predominantly alpha-type but with difference in the amount of nitrate incorporation. In turn this nitrate incorporation produces some interesting structural results, which are expected to provide more understanding towards anion-substituted hydroxides. The results are interesting in terms of interlayer distances and faradaic efficiency of the material synthesis.

EXPERIMENTAL SECTION

Electro-deposition of nickel hydroxide samples was carried out in open air atmosphere on platinum and nickel substrates by cathodic electrolysis of 0.1 M $Ni(NO_3)_2$ solutions prepared from conductivity water (Millipore). In a typical electro synthesis experiment a nickel plate of geometric area, 40 cm^2 (both sides) was cleaned and dried to be used as a working electrode substrate. The substrate and a platinum-plate counter electrode were immersed in a stirred solu-

tion of 750 ml of 0.1 M $Ni(NO_3)_2$ (pH=4.69) maintained at 30.00 °C by temperature controller (Julabo-Model-FP40). Subsequent to one minute after immersion, the substrate was cathodicaly polarized by passing a galvanostatic current of 40 mA for 10 hours i.e. a charge of 400 mAh with the aid of computer controlled multichannel potentiostat-galvanostat (VMP2- Princeton applied Research). The stirring and temperature control were well maintained during the course of the entire experiment. Immediately after the end of the experiment, the substrate which turned transparent-crystalline green in appearance due to the reasonably-adherent deposit was removed from the electrolyte solution and repeatedly washed with conductivity water for several times. Then the green deposit was removed by dry air at 40 °C. The collected green powder was dried for 24 hours at 65 °C in hot-air-oven and the samples were weighed accurately to calculate the yield and faradaic efficiency.

Further electro-synthesis experiments were carried out in fresh $Ni(NO_3)_2$ solutions under similar conditions with currents of 200 mA, 240 mA, 280 mA and 400 mA for 2 h, 1.6 hr, 1.26 hr and 1 hour respectively thus maintaining the total charge of 400 mAh. Thus the current densities of the electrodeposition experiments were 1.0, 5.0, 6.0, 7.0 and 10.0 $mAcm^{-2}$. Another set of similar experiments were carried out with platinum plate as substrate with the remaining parameters unaltered. Thus 10-samples were systematically prepared for this study (*Table* 1).

The samples were adhered to silver paste and dried for electrical contact to observe SEM pictures. Elemental analysis (EDAX) of the samples was performed in Hitachi scanning electron microscope (SEM S-4200). The experiments were mainly aimed at finding out the percentage content of carbon arising from carbonate ions.

Infra red spectral data of the nickel hydroxide samples were collected at 25 °C in FTIR spectrometer (Nicolet Instruments Corporation) provided with data analysis software (Ominc-3.1). Portemer et. al. have suggested the usage of CsI instead of conventionally used KBr as dispersion medium to reduce the loss of IR signal intensity and resolution with regard to nitrate ion. In the present experiments, the samples for the IR spectroscopy experiments consisted of pressed circular pellets. A typical circular pellet was prepared by mixing and grinding 4 mg of nickel hydroxide and 196 mg of CsI followed by compaction at 4 tons load for 10 seconds. The resulting pellet possessed the dimensions of 12.86 mm diameter and 0.85 mm thickness with the IR exposure area being the 0.6 cm^2 around the center. Identical pellets were prepared for all the 10-samples for effective comparison.

X-ray diffraction experiments were carried out in Rigaku-Japan diffractometer (Model D/max, Rint 2000) with Cu-K-Alpha radiation (wave length=1.5418 A) as source at a scan rate of 1 deg / min in the two-theta range 5°–70°. TGA and DSC data were col-

Table 1. Experimental conditions employed for the electrodeposition, amount (mass) of the deposit and calculated faradaic efficiencies of the α-nickel hydroxide samples. In all the experiments the total charge passed is equal to 400 mAh.

Substrate	Ser. No.	Sample name	Current density $mAcm^{-2}$	Duration Hr:m	Amount deposited (gms)	Faradiac efficiency (%)
Platinum plate (40 cm^2 total area)	1	Pt-01	1.0	10:00	0.2905	37.0
	2	Pt-05	5.0	2:00	0.5266	67.2
	3	Pt-06	6.0	1:40	0.4592	58.6
	4	Pt-07	7.0	1:26	0.5453	69.6
	5	Pt-10	10.0	1:00	0.5741	73.3
Nickel Plate (40 cm^2 total area)	6	Ni-01	1.0	10:00	0.2945	37.6
	7	Ni-05	5.0	2:00	0.4776	61.0
	8	Ni-06	6.0	1:40	0.4238	54.1
	8	Ni-07	7.0	1:26	0.4789	61.1
	10	Ni-10	10.0	1:00	0.4433	56.6

lected at the scan rate of 5 °C per min in TA instrument, USA (model: DSC 2920 and TGA 2050).

Temperature programmed desorption (TPD) studies were carried out in the gas chromatography instrument coupled with mass spectrometer (GC-MS) analyzer connected to the sample holder.[12] In a typical experiment 100 mg of the sample was introduced into the bottom of the U-shaped sample tube which was heated by a furnace and the temperature of the sample was measured accurately with the help of a Pt-Rd thermocouple. Helium at a pressure of 6.5 psi was used as the carrier gas to carry the desorbed species at instant of time. The temperature of the GC column was maintained at 250 deg C for fast and effective movement of the desorbed species towards the MS analyzer. The sample was preheated and degassed for 1 hour at 65 deg C and the temperature was increased at the rate of 5° per minute up to 700 °C. At regular intervals of time (and hence temperature) the desorbed species were detected by the mass spectral analyzer which results in the ion-spectrum which is the plot of ion-current vs temperature. Details regarding desorbed species at each temperature were obtained by deconvolution of the ion-spectrum from the knowledge expected species of known mass numbers. The amount of such species desorbed from the sample over the temperature range 65-700 °C was obtained as a graph and it is called the individual species spectrum. The amount of each species in unit mass of the sample is quantified by integrating the individual species spectrum over the entire temperature range. Additionally, if the same species is desorbed at more than one instance they can be individually integrated over the short temperature range to understand the source of the species. This would be more clearly understood with a representative example in the results and discussion section.

The attempts to synthesize CO_3^{2-} (carbonate-free) samples failed due to the extreme difficulty faced in the production of CO_2-free water. Although experimental reports are suggesting the preparation of CO_2-free water by purging argon, we found the method not be satisfactisfactory as our synthesis can include CO_3^{2-} ions even when present in ppm levels. In future these expements could be planned with such conditions.

RESULTS AND DISCUSSION

All the electro-deposits were reasonably adherent and crystalline green in appearance, which got detached by drying at 40 °C, which suggests the absence of any chemical bonding between the sam-

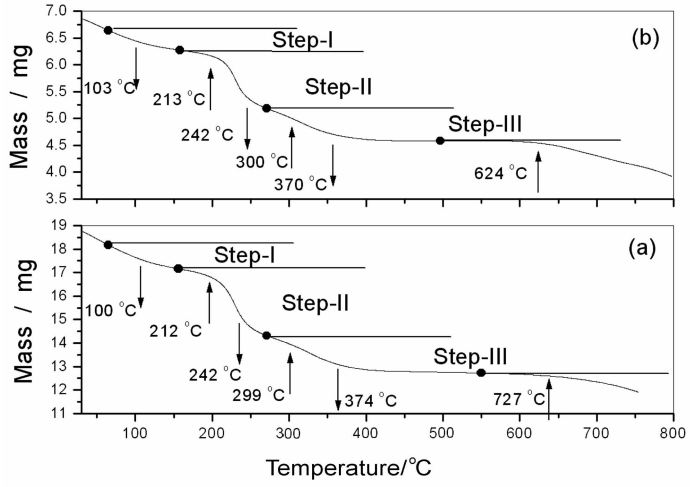

Fig. 1. TGA data of $Ni(OH)_{2-x}(CO_3)_{x/2}(NO_3)_x.zH_2O$ samples electrodeposited at a current density of 6.0 mA cm^{-2} on (a) platinum substrate and (b) nickel substrate. (↑ refers to upward curvature and ↓ refers to downward curvature and • refers to midpoint).

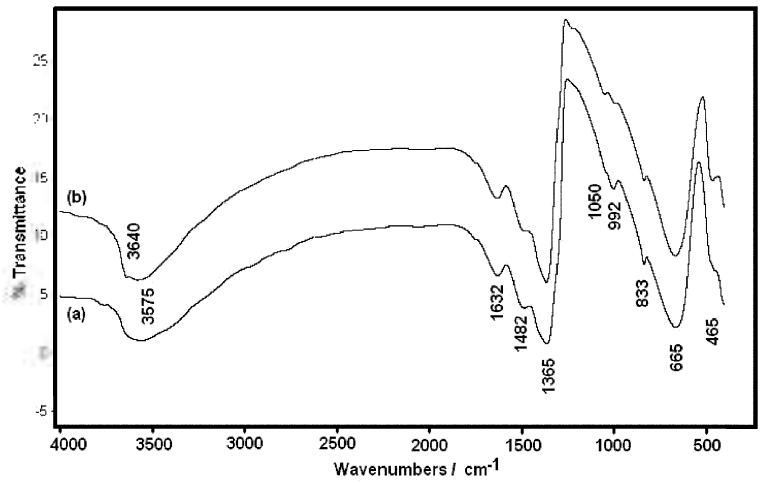

Fig. 2. FTIR spectra of the electrodeposited $Ni(OH)_{2-x}(CO_3)_{x/2}(NO_3)_x.zH_2O$ samples (a) on platinum at 5 mAcm^{-2} (resulted in x-value = 0.1332) and (b) on nickel at 1 mAcm^{-2} (resulted in x-value = 0.2022).

ple and substrate. The mass of the nickel hydroxide deposit obtained for a constant input charge of 400 mAh over nickel and platinum substrates for various current densities are tabulated in *Table* 1. The calculated faradaic efficiencies will be understood upon reading the later section of the article.

The elemental analyses show the samples to consist of nickel, oxygen, hydrogen carbon and nitrogen. This suggests that the samples must contain carbonate and nitrate. The elucidation of the anions will be the main study of this manuscript. The TGA data of two representative samples are shown in *Fig.* 1. But the curves do not show clear and differentiable steps to determine the composition.

The infrared spectral data of two samples as typical examples are shown in *Fig.* 2. The spectra of all the ten samples studied are similar over the entire infrared range except for the broad band region around 3500 cm^{-1}. In general the spectra show the following absorption signals provided along with the assignments: The signals at 465 cm^{-1} due to (stretching vibrational modes) γ(NiO), 664 cm^{-1} for (bending vibrational modes) δ(OH) 1632 cm^{-1} due to δ(H_2O) are assigned unambiguously.[12]

The presence of carbonate ions are confirmed from the signal at 1048 cm^{-1} arising due to g(CO_3^{2-}) with c_2v symmetry and the strong signal at 1365 cm^{-1} due to the carbonate g(CO_3^{2-}). The appearance of signal at 833, 992 and 1482 cm^{-1} agrees with carbonate as well as nitrate ions in d_3h and c_2v symmetry. The signals appearing the in the range 3500-3600 cm^{-1} which are responsible for the OH stretching vibrations under various situations are very interesting and will be discussed towards the end of this manuscript.

The X-ray diffraction patterns of the samples are shown in *Figs.* 3 and 4. From a broad appearance all the samples look to crystallize in similar α-nickel

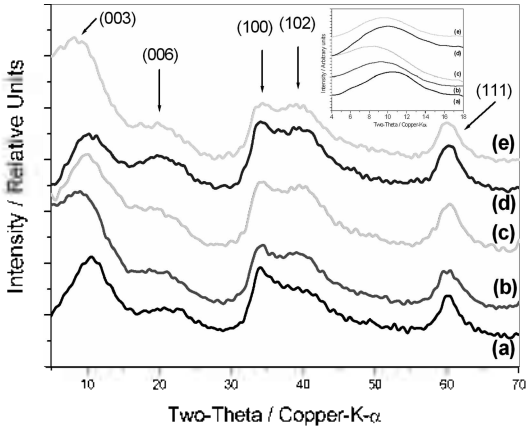

Fig. 3. Powder XRD patterns of $Ni(OH)_{2-x}(CO_3)_{x/2}(NO_3)_x.zH_2O$ electrodeposited deposited on platinum substrate at current densities of (a) 1.0 mA cm^{-2}, (b) 5.0 mA cm^{-2}, (c) 6.0 mA cm^{-2}, (d) 7.0 mA cm^{-2}, (e) 10.0 mA cm^{-2}. The inset shows the peak positions of 003 reflections.

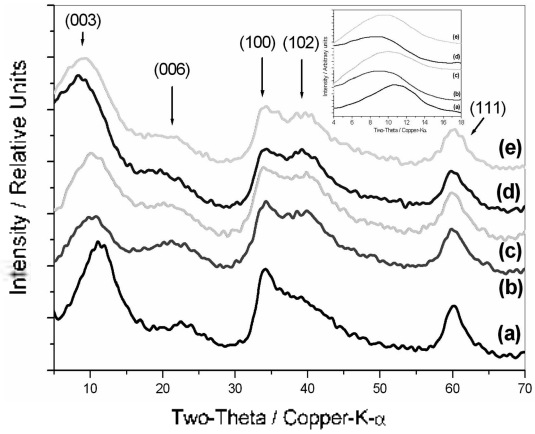

Fig. 4. Powder XRD patterns of $Ni(OH)_{2-x}(CO_3)_{x/2}(NO_3)_x.zH_2O$ samples deposited on nickel substrate at current densities of (a) 1.0 mA cm^{-2}, (b) 5.0 mA cm^{-2}, (c) 6.0 mA cm^{-2}, (d) 7.0 mA cm^{-2}, (e) 10.0 mA cm^{-2}. The inset shows the peak positions of 003 reflections.

hydroxide structure. The asymmetry of the higher angle peaks shows additional proof for the formation of turbostratic structures peculiar to α-nickel hydroxide.[13] But, when closely analyzed the corresponding 003 lines are shifted to higher angles upon increase in current density which is very prominent in samples deposited on nickel substrate than those deposited on platinum substrate as shown in *Figs.* 3 and 4. The 003 lines arise from the layers of nickel hydroxide perpendicular to the c-axis of the lattice and hence it is a measure of the interlayer spacing. The XRD patterns were accurately indexed to obtain the lattice parameters of hexagonal unit cell of α-nickel hydroxide. The lattice parameters of all the samples are listed in *Table* 2. From the lattice constants provided in *Table* 2 and a view at the diffraction patterns it is clear that lattice expansion occurs for the materials deposited at higher current densities with retention of similar structure. Although the broad peaks indicate smaller crystallite size, reliable values of sizes could not be obtained by debye-sherrer formula due to turbostraticity. Roughly we describe the sample to consist of positively charged hydroxyl deficient nickel hydroxide layers with the charge balanced by the anions in between the layers namely carbonates and nitrates. In turn the amount of these anions change the interlayer distances. The factors responsible for the change in interlayer spacing will be understood with the aid of the chemical composition determined with thermal analysis. The a-lattice parameter remains unchanged around 3.1 A° for all the samples. The c-lattice parameter increases with current density for sample deposited on nickel-substrate, while as such an effect is not observed for samples deposited on platinum substrate.

Apart from the increase change in the c-lattice parameter, it is noteworthy to point out that some samples such as pt-10, pt-05, Ni-10, Ni-07 show very large c-lattice constant values around 27-28 Angstroms which equates to an interlayer (interlamellar) distance of ~9.4 A°. A similar observation with regard to high lattice interlayer distance has been observed by Ismail et al.[14] They observed a interlayer distance of 9.3 A° corresponding to the 001 reflection

Table 2. The Unit cell parameters and stoichiometry of the electrodeposited $Ni(OH)_{2-x}(NO_3)_x.y\ H_2O$ samples obtained on platinum and nickel substrates at various current densities.

Substrate	Current density $mAcm^{-2}$	Sample Name	"a" Angstroms	"c" Angstroms	x-value of the chemical formula	y-value of the chemical formula	Final molecular weight
Platinum	1.0	Pt-01	3.0883	24.942	0.1675	0.3856	107.167
	5.0	Pt-05	3.0939	28.380	0.1332	0.3095	104.255
	6.0	Pt-06	3.0977	26.958	0.1454	0.3211	105.012
	7.0	Pt-07	3.1005	26.982	0.1559	0.3036	105.170
	10.0	Pt10	3.0743	28.467	0.1363	0.2691	103.667
Nickel	1.0	Ni-01	3.1005	23.826	0.2022	0.3313	107.753
	5.0	Ni-05	3.0855	25.194	0.1725	0.3341	106.466
	6.0	Ni-06	3.0958	26.325	0.1715	0.3291	106.331
	7.0	Ni-07	3.0930	27.036	0.1532	0.3104	104.292
	10.0	Ni10	3.0864	27.564	0.1480	0.3495	105.640

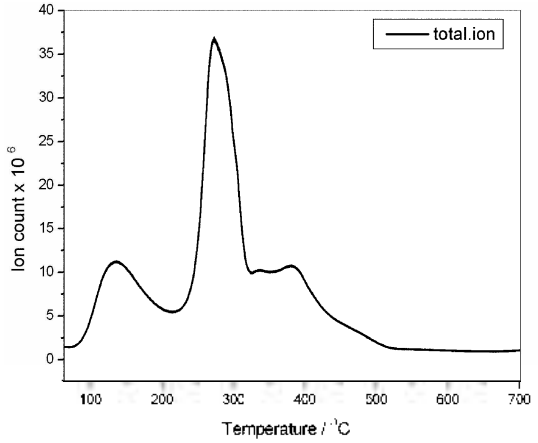

Fig. 5. Temperature programmed Desorption (TPD) data of $Ni(OH)_{2-x-y}(CO_3)_{x/2}(NO_3)_y.zH_2O$ sample deposited on nickel substrate at current densities of 5.0 mA cm^{-2}. The ion-count represents the ion-current signal obtained at each temperature from the mass spectrometer.

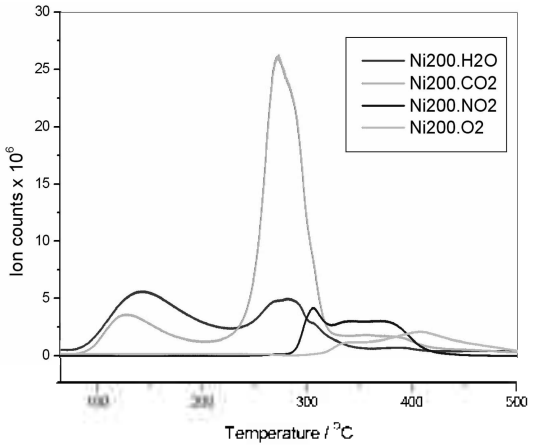

Fig. 6. Individual-species TPD spectrum for the $Ni(OH)_{2-x-y}(CO_3)_{x/2}(NO_3)_y.zH_2O$ sample deposited on nickel substrate at current densities of 5.0 mA cm^{-2}. The data is obtained by the deconvolution of the data presented in *Fig.* 4.

of malice acid intercalated $Co(OH)_2$ phase. But that phase is β-$Co(OH)_2$ with interlayer distance corresponding to c-lattice parameter. This is the one noteworthy reference with respect to high interlayer spacing. This is a first time observation and is unexpected as the usual interlayer distances are around 7.5 A° with the intercalated anions being nitrates. We suspected the large interlayer distance could possibly arise from carbonate ions and nitrate ions present in large numbers and sitting in special configurations. In order to understand this point we have performed a temperature programmed GC-MS experiments.

The temperature programmed GC-MS experiments yield the ion spectrum and from them individual species spectrum could be obtained. A typical ion-spectrum of a sample is shown in *Fig.* 5. The figure shows the sample to consist of huge amount of desorbable specie. In detail, the peak signal values are 11 million at 137 deg C, 36 million at 273 deg C, 10 million at 336 and 10.7 million at 380 °C. The sample becomes thermally stable beyond 520 °C. Since the sample is supposed to be hydroxy deficient nickel hydroxides, all thermally desorbable species get removed and the sample gets converted to nickel oxide at 520 °C. We are more interested in the analyzing the spectrum up to 500 °C since we plan to investigate the nature and magnitude of the desorbable species and their source.

Since the preliminary investigation such as IR and XRD show the samples to consist of carbonate and nitrate ions intercalated in the nickel hydroxide, the molecular ions arising from four species namely H_2O, CO_2, NO_2 and O_2 could be expected to be the cause for the total ion-spectrum. This is also confirmed from the MS spectra result which suggests molecular ions with mass numbers 18, 44, 46 and 32 are only produced and they result from H_2O, CO_2, NO_2 and O_2 respectively. *Fig.* 6 presents the data consisting of four deconvoluted indivual species spectra.

The following processes are responsible for the production of afore mentioned sepecies of desorption:

Process 1:

$$H_2O_{\text{(in between the layers)}} \xrightarrow{\text{Thermal Desorption}} H_2O_{(gas)} \xrightarrow{\text{followed by ionization}} \rightarrow H_2O_{\text{(molecular ion of mass 18)}}$$

Process 2

$$CO_3^{2-}\ \text{(intercalated)} \xrightarrow{\text{Thermal Desorption}} \rightarrow CO_{2(gas)} + O^{2-}_{\text{(remains in the sample)}}$$

$$CO_{2(gas)} \xrightarrow{\text{followed by ionization}} CO_{2\text{(molecular ion of mass 44)}}$$

Process 3

$$NO_3^- \text{ (intercalated)} \xrightarrow{\text{Thermal Desorption}} NO_{2\,(gas)} + \tfrac{1}{2}O^{-}_{\text{(remains in the sample)}}$$

$$O^{-}_{\text{(remains in the sample)}} \xrightarrow[\text{ionization}]{\text{followed by}} O_{2\,\text{(molecular ion of mass 46)}}$$

Process 4

$$Ni(OH)_2\text{(substrate)} \xrightarrow{\text{Thermal Desorption}} H_2O_{(gas)} + NiO_{(solid)}$$

$$H_2O_{(gas)} \xrightarrow[\text{ionization}]{\text{followed by}} H_2O_{\text{(molecular ion of mass 18)}}$$

The data shows that major contribution of ion-current arises from the carbonate ions present in the sample followed by H_2O molecules then followed by nitrate ions. Contrary to the usual description of alpha-nickel hydroxide samples these samples are found to consist of carbonate ions in excess as compared to nitrate ions. So far in the literature the presence of carbonate ions is neglected and we would like to add this new finding for the future references. With regard to the nature of the carbonate ion, they are released at temperatures of 125 and 280 °C with a majority coming from 280 °C. The nitrate ions are present in small amount as compared to carbonate ions but they are released at higher temperature. This shows that the nitrate ions are more strongly bonded to the lattice than carbonate ions as shown by the desorption temperature.

The amount of CO_3^{2-}, NO_3^- and H_2O molecules are calculated from the integral area of the individual-species spectra. These integral values were further processes to the get the x, y and z of the formula unit of $Ni(OH)_{2-x-y}(CO_3)_{x/2}(NO_3)_y.zH_2O$. The samples consisted of large but unvarying x value and unvarying z value. But the "y" value i.e. the nitrate content changes in a special fashion over the samples. A plot of the nitrate ion-content vs. the lattice constant obtained for various samples is presented in *Fig.* 7. It is observed from the figures the interlayer spacing increases with the decreasing content of nitrate ions. The influence of carbonate ions towards the change in lattice constant is minimum as it is present is large excess (30 million). Whereas the nitrate ions are present is small amount (10 million) and their

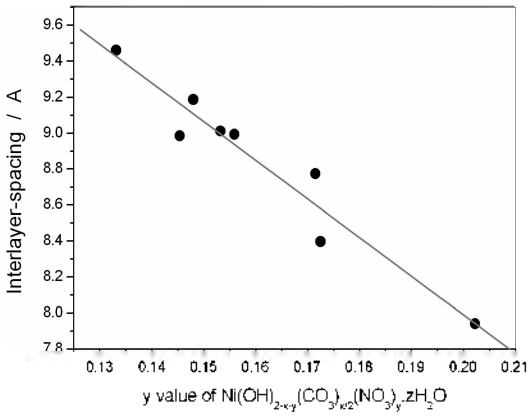

Fig. 7. The variation of interlayer spacing with the y-value of the chemical formula, $Ni(OH)_{2-x-y}(CO_3)_{x/2}(NO_3)_y.zH_2O$.

halving causes a significant increase in the lattice spacing although the carbonate ions is present in excess. The formula of these phases are correctly given by $Ni(OH)_{2-x-y}(CO_3)_{x/2}(NO_3)_y.zH_2O$. We could consider the fundamental phase to be $Ni(OH)_{2-x}(CO_3)_{x/2}.zH_2O$ and the nitrate substitution to result in double-anion substituted phases. The study of purely single anion substituted phases are difficult due to experimental problems arising out of (i) preparation of ultra pure CO_2-free water which could result in $Ni(OH)_{2-y}(NO_3)_y.zH_2O$ phases and (ii) availability of suitable electrochemical methods to form $Ni(OH)_{2-x}(CO_3)_{x/2}.zH_2O$ phases. Carbonate ions are incorporated during the chemical precipitation reaction solution consisting nickel and aluminium nitrate and alkali producing $Ni_{1-x}Al_x(OH)_2(CO_3)_{x/2}.zH_2O$ type of phases.[8] The experiments to synthesize such ordered phases are under progress.

We quantify the above observed lattice contraction of interlayer contraction by the nitrate ions by the couloumbic attraction between interlayer-anions and the positively charged hydroxyl deficient slabs. Similar observation was made by Rhee and Kang in Mg-Al-layered double hydroxides with carbonate ions as intercalated anions. They observed interlayer spacing of 7.90, 7.82 and 7.65 Å for carbonate ion contents (x values) of 0.196, 0.250 and 0.326 in $Mg_{1-x}Al_x(OH)_2(CO_3)_{x/2}$ phases[15]. But the between those results and ours are the ions responsible for

the coulumbic effect, viz. nitrates are responsible in the anion-substituted α-nickel hydroxide phases as against carbonates in the Mg-Al-LDH phases. In the light of these above findings by the GC-MS experiments which give a clear picture of the nature of anions and their amount would explain the lattice contraction effect. It is felt unnecessary to discuss the results of the TGA data as the discussion involves several predictions when weight loss steps merge as in the case of present samples.

The electrostatic force between the positively charged slab and intercalant could be expressed by the following expression:

$$\text{Coulumbic attractive force} = \frac{K*y^2}{\text{Interlayer spacing}^2} \quad (1)$$

where "y" refers to the partial ionic charge of the positively charged slab which is also equal to the total anionic charge. For small variation in the amount of intercalated anions the change in columbic force could be considered negligible and the above expression reduces to an easy form,

$$\text{Interlayer spacing} - \text{slope}* \text{y-value in } Ni(OH)_{2-x-y}(CO_3)_{x/2}(NO_3)_y.zH_2O \quad (2)$$

A plot of the amount of intercalated nitrate ions per mole vs. inter layer spacing is provided in *Fig.* 7. The plot is a straight line with a negative slope and it confirms the hypothesis that excess anions bring the positively charged slabs closer. Moreover the effect is brought only by nitrate ions and not carbonate ions although carbonate ions are present is large excess. A possible explanation for this effect could be the tightly bonded nature of nitrate ions as observed from higher desorption temperature in the GC-MS data.

The lattice contraction effect is further augmented by the FTIR signals arising out of the OH stretching vibrations in the range 3500-3600 cm^{-1} for the hydroxyl groups of nickel-hydroxide slabs. A family of FTIR curves in the range 3500-3600 cm^{-1} for all the samples arranged according to increasing amounts of nitrate ions is provided in *Fig.* 8. The

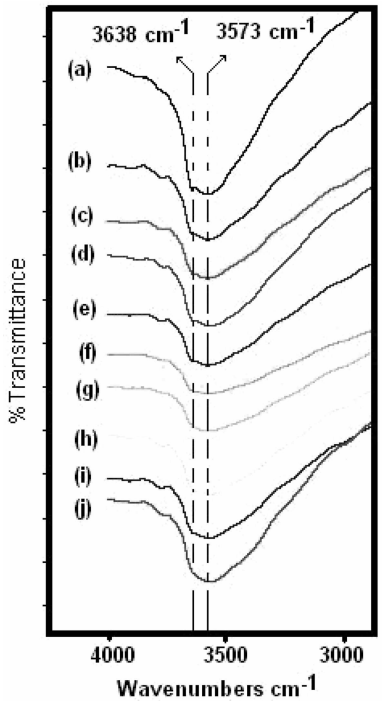

Fig. 8. FTIR spectra of the $Ni(OH)_{2-x-y}(CO_3)_{x/2}(NO_3)_y.zH_2O$ samples arranged in the increasing order of "x" values from (a) to (j) with sample and "y" values as follows: (a) Pt-05; y=0.1332, (b) Pt-10; y=0.1363, (c) Pt-06; y=0.1454, (d) Ni-10; y=0.1480, (e) Ni-07; y=0.1532, (f) Pt-07; y=0.1559, (g) Pt-01; y=0.1675, (h) Ni-06; y=0.1715, (i) Ni-05; y=0.1725 and (j) Ni-01; y=0.2022.

samples with larger content of nitrate ions show a smooth broad band and asymmetric band centered around 3560 cm^{-1} whereas the samples with smaller content of nitrate ions show an additional sharp peak around 3640 cm^{-1}. Indeed the 3640 cm^{-1} signal becomes less and less visible for samples with high nitrate ions contents. In literature the band around 3560 cm^{-1} is attributed to stretching vibration of OH group hydrogen bonded to nitrate ions where as the band at 3640 cm^{-1} is attributed to stretching vibration of free OH groups. The samples with higher nitrate ions have only 3560 cm^{-1} signal indicating all the OH bonds are strongly associated with nitrate ions through hydrogen bonds, which could be either the cause for lattice contraction or result of lattice contraction. An exact reverse behavior is observed in the samples with lower content of nitrate ions,

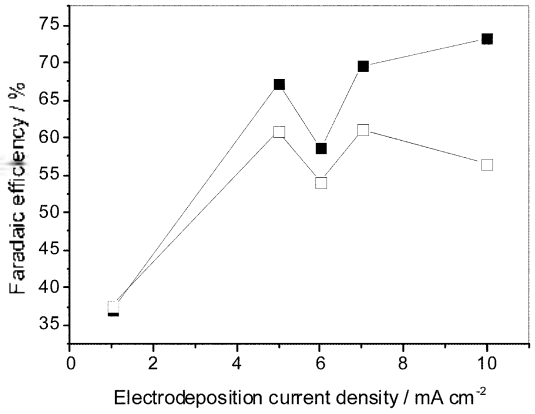

Fig. 9. Effect of electrodeposition current density on results of the $Ni(OH)_{2-x-y}(CO_3)_{y/2}(NO_3)_x.zH_2O$ samples in their (a) "a" lattice parameter, (b) "c" lattice parameter, (c) "x" value of the chemical formula, (d) "y" value of the chemical formula and (e) faradaic efficiency of synthesis. Note: Filled-symbols for samples deposited on platinum and open-symbols for samples deposited on nickel substrate.

where free OH IR signal is observed which indicates that interlayer spacing is large enough to allow some of the OH groups to be free. A gradation in lattice contraction results in the diminishing existence of free OH groups.

Fig. 8 shows an increase in faradaic efficiency with applied current density for both platinum and nickel substrates in a similar trend from 1 to 10 $mAcm^{-2}$. A mathematical model for the galvanostatic deposition of nickel hydroxide is proposed by Weidner et. al..[16] In that work, the efficiency of electrodeposition is well explained with respect to change of current density. Several electrochemical as well as chemical reactions were considered as part of the beginning building blocks, but the weight of nickel hydroxide deposit, which leads to calculation of faradaic efficiency depends on the following reactions:

$$Ni^{2+} + 2\,OH^- \rightarrow Ni(OH)_2 \downarrow \quad (3)$$

$$Ni^{2+} + OH^- \rightarrow \tfrac{1}{4}\,Ni_4(OH)_4^{4+} \quad (4)$$

$$\tfrac{1}{4}\,Ni_4(OH)_4^{4+} \rightarrow Ni(OH)_2 \downarrow \quad (5)$$

It is clear from the above chemical equations that the concentration of OH^- ions decides the amount of deposit. From these considerations a final expression was derived for the weight of nickel hydroxide deposited as:

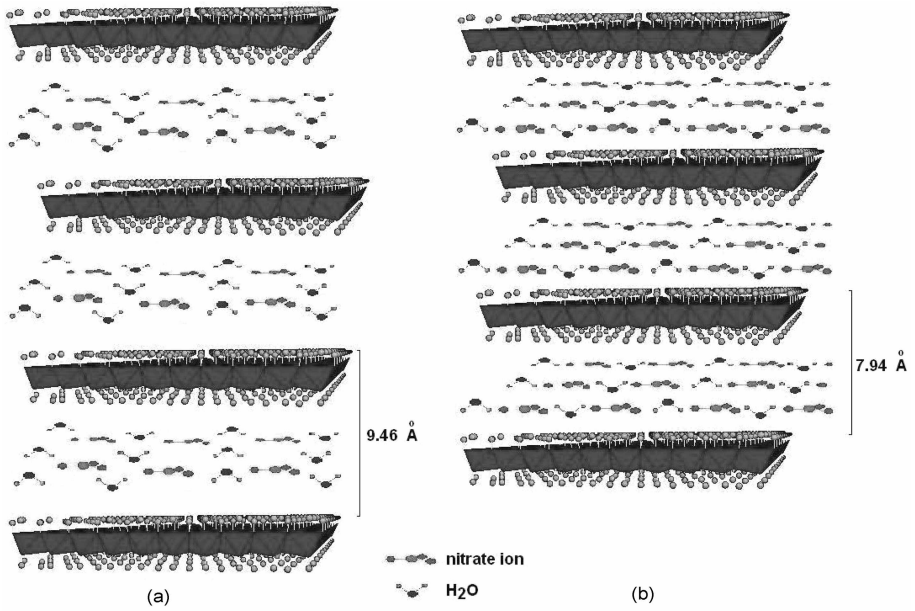

Fig. 10. Schematic representation of (a) Pt05 i.e., $Ni(OH)_{2-x-y}(CO_3)_{y/2}(NO_3)_x.zH_2O$ (y=0.1322) and (b) Ni01 i.e., $Ni(OH)_{2-x-y}(CO_3)_{y/2}(NO_3)_x.zH_2O$ (y=0.2022) showing the lattice contraction of hydroxy deficient layers by anions.

$$W_{Ni(OH)2} \propto \frac{9iAW_{Ni(OH)2}\,\varepsilon_{OH^-}}{16F} \qquad (6)$$

where, i is the applied current density, $W_{Ni(OH)2}$ is the molecular weight of the deposit, ε_{OH^-} efficiency of utilization of OH^- ions, A is the geometric area and F is the faraday constant. It is very much expected from expression (6) that the faradaic efficiency which is the ratio of actual weight to the expected weight is directly proportional to the current density and hence the observed behavior of increase in faradaic efficiency with current density is well understood. Mechanistic studies are still in progress to reason out the superior faradaic efficiency of platinum over nickel substrates.

CONCLUSIONS

In this study it is demonstrated that an interesting effect is produced in the interlayer spacing for α-nickel hydroxide upon varying the electrodeposition current density close to 5.0 $mAcm^{-2}$. The response of platinum substrate towards a small change in current density is very prominent in producing a change in interlayer spacing of alpha nickel hydroxide. We have demonstrated that the nature of nitrate ion and hence its amount is the deciding factor in bringing lattice contraction through its columbic attractive force upon the adjacent positively charged hydroxy-deficient slabs. In the literature the effect of size of ion on the lattice spacings and hence the properties had been demonstrated.[17] We hope to look at these interesting aspects in future. The faradaic efficiency of deposition on platinum substrate is marginally higher than nickel substrate which is attributed to some amount of charge consumed for corrosion of nickel substrate. The response of various parameters including faradaic efficiency at the crucial current density of 6.0 $mAcm^{-2}$ is interesting and it is under further investigation.

GC-MS analysis of the electrodeposited nickel hydroxide samples show that the major proportion anions are carbonate ions and minor proportion comes from nitrate ions. This is a new observation as the samples are usually assumed to be nitrate containing samples. Further the GC-MS experiments clearly demonstrate that the nitrate ions are strongly bonded in between the positively charged layers as compared to the carbonate ions as inferred from the temperature of their elimination. Such a demarcation is not possible with usual TGA analysis.

Acknowledgements. This work was financially supported by the Ministry of Education and Human Resources Development (MOE), the Ministry of Commerce, Industry and Energy (MOCIE) and the Ministry of Labor (MOLAB) through the fostering project of the Lab of Excellency. One of the authors, V. Ganesh Kumar, would like to thank the Korean Federation of Science and Technology (KOFST), Seoul, Korea, for offering a Brain Pool Visiting Fellowship.

REFERENCES

1. D. Linden (Ed.) Handbook of Batteries, McGraw Hill, New York, **1995**.
2. Kumar, V.G.; Shaju, K.M.; Munichandraiah, N.; Shukla, A.K. *J. Power Sources*, **1998**, *76*, 106.
3. Tessier, C.; Haumesser, P.H.; Bernard, P.; Delmas, C. *J. Electrochem. Soc.* **1999**, *146*, 2059.
4. Carpenter, M.K.; Conell, R.S.; Corrigan, D.A. *Solar Energy Materials* **1987**, *16*, 333.
5. Corrigan, D.A.; Knight, S.L. *J. Electrochem. Soc.* **1989**, *136*, 613.
6. Singh, D. *J. Electrochem. Soc.* **1998**, *145*, 116.
7. Kumar, V.G.; Munichandraiah, N.; Kamath, P.V.; Shukla, A.K. *J. Power Sources* **1995**, *56*, 111.
8. Kamath, P.V.; Dixit, M.; Indira, L.; Shukla, A.K.; Kumar, V.G.; Munichandraiah, N. *J. Electrochem. Soc.* **1994**, *141*, 2956.
9. Dixit, M.; Jayashree, R.S.; Kamath, P.V.; Shukla, A.K.; Kumar, V.G.; Munichandraiah, N. *Electrochem. and Solid State Letters*, **1999**, *2*, 170.
10. Jayashree,R.S.; Kamath, P.V. *J. Applied Electrochem.* **1999**, *29*, 449.
11. Portemer, F.; Delahaye-Vidal, A.; Figlarz, M. *J. Electrochem. Soc.* **1992**, *139*, 671.
12. Jung, K.T.; Kim, W.B.; Rhee C.H.; Lee, J.S. *Chem. Mater.* **2004**, *16*, 307.
13. Genin, P.; Delahaye-Vidal, A.; Portemer, F.; Tekaia-Elhsissen, K.; Figlarz, M. *Eur. J. Solid State Inorg. Chem.* **1991**, *28*, 505.

14. J. Ismail, M.F. Ahmed, P.V. Kamath, G.N.Subbanna, S. Uma and J. Gopalakrishnan *J. Solid State Chem.* **1995**, *114*, 550.
15. Rhee, S.W.; Kang, M.J. *Korean J. Chem. Eng.* **2002**, *19*, 653.
16. Murthy, M.; Nagarajan, G.S.; Weidner, J.W.; VanZee, J.W. *J. Electrochem. Soc.* **1996**, *143*, 2319.
17. Taibi, M.; Ammar, S.; Jouini, N.; Fievet, F.; Molinie, P.; Drillon, M. *J. Mater. Chem.* **2002**, *12*, 3238.